

<Original>

## Structure of Premixed Turbulent Flames Stabilized by a Cylindrical Flame Holder†

Byeong Ryun Choi\*, Masashi Katsuki\*\* and Yukio Mizutani\*\*

(Received March 9, 1985)

圓柱 保焰器에 의해 安定化된 亂流 豫混合 火焰의 構造

崔 炳 輪 · 香月 正司 · 水谷 幸夫

**Key Words:** Combustion(연소), Premixed Flame(예혼합화염), Coherent Structure (코히런트 구조), Shear Layer(전단층)

### 초 록

일양한 예혼합 기류중에 놓여진 원주 후류의 고온 순환류에 의해 보지되는 난류 예혼합 화염을 대상으로 해서 유동의 가시화 및 온도와 이온전류의 변동의 측정에 의해서 화염의 구조를 조사한 결과, 원주 보염기 후류의 재순환 영역부근에 형성된 전단층에 있어서는 코히런트(Coherent)구조의 화염이 되고 하류부에서는 불규칙한 3차원 와(渦)에 지배되는 전파성 화염이 형성 되었다. 온도변동에 대한 쌍봉성의 확률밀도분포와 이온전류변동에 대한 3개의 피이크의 확률밀도분포는 얇은 반응면을 사이에 두고 미연혼합기피와 기연가스피가 서로 접하는 주름 상층류화염 또는 층류화염면의 구조에 대응하며, 코히런트 와(渦)에 지배되는 화염에 있어서는 거시적 혼합은 코히런트 와의 거동에 지배되나 그 구조는 주름상층류 화염과 일부 강한 전단력을 받는 부분에는 분산 반응영역의 구조임이 밝혀졌다.

### 1. Introduction

The flame stabilization by a flame holder has often been utilized in practical combustion devices, and extensive experimental and theoretical studies on the mechanism of flame stability have been published<sup>(1~7)</sup>.

In most of them, the mechanism is discussed

based on the time-averaged values of turbulent exchange or of heat balance. On the other hand, some observations pointed out that large scale fluctuations of a flame front dominate the blowout or flashback behavior of flames<sup>(8~10)</sup>.

Although the discussions based on the time-averaged values may be applicable when the flame is stably stabilized it is essential to know the structure of turbulence and fluctuations of scalar properties because instantaneous conditions should be considered for the discussion of limiting processes such as blowout. Some experimental studies concerning the measurements

† Presented at the 1983 ASME-JSME Joint Thermal Engineering Conference

\* Member, Dept. of Mechanical Engineering, Pusan National University

\*\* Professor, Dept. of Mechanical Engineering, Osaka University

of fluctuations have been reported recently<sup>(11,12)</sup>, and more extensive studies to elucidate the structure of turbulent flames are expected.

In the present study, to obtain the fundamental information about the structure of premixed flames stabilized by a cylinder, flow visualization and time-resolved measurements of fluctuations of temperature and ion concentration have been made, and statistical properties have also been examined.

## 2. Experiments

Figure 1 shows the main parts of experimental setup. Optical observations were carried out through vycor side walls of combustion tunnel of a rectangular cross section (100mm × 30mm) provided with a water cooled (ca. 330K) cylindrical flame holder of 20mm in diameter. The stabilized flame is two dimensional in macroscopic, and  $x$ - $y$  coordinates are settled having their origin at the center of the cylinder as shown in Fig. 1. All measurements were made in the central plane between two vycor walls. Approach turbulence intensity can be varied by changing the turbulence grid (Type I : Wire screen, Type II : Perforated plate) inserted 145mm upstream of the cylinder. A regulated town gas (natural gas)/air mixture of equivalence ratio  $\phi$  is supplied as the combustible mixture. Nominal flow velocity  $U$  is defined as the value of volumetric flow rate divided by the actual area of  $x=0$ mm cross section.

A conventional schlieren arrangement, consisting of two concave mirrors and a knife edge, and spark photographs ( $<1\mu\text{s}$ ) or high speed movies (max. 5000fps) were used to record the images.

The measuring system is shown in Fig. 2. The thermocouple employs  $25\mu\text{m}$  platinum/

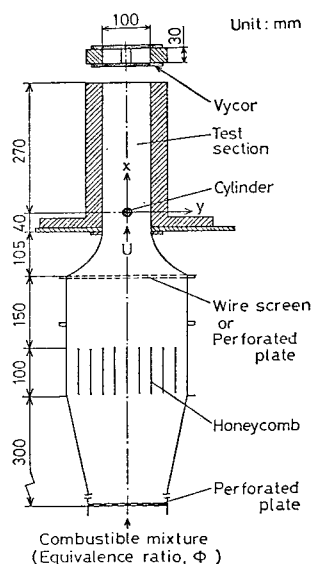


Fig. 1 Experimental apparatus

platinum 13% rhodium bare wire combinations. The deterioration in frequency response caused by the effects of thermal inertia is compensated electrically. In order to determine the local time-averaged time constant  $\tau$  of compensation, several methods such as a heat balance method<sup>(13)</sup> or a step response method<sup>(14)</sup> are found in the literature. However, each of them has merits and demerits when local properties of flow conditions are not known or taking into account the inaccuracy in the measurements of local time-averaged time constant. In the present study, the method was adopted in which time constant was selected such that the distributions of the PDF of temperature fluctuations be appropriate<sup>(15)</sup>, because a lot of attention will be focussed on the shape of probability density function which characterizes the flame structure.

For the measurements of fluctuating ion concentration, an electrostatic probe of 0.1mm in diameter and 0.5mm in length was used. Simultaneous measurements of temperature and ion concentration were carried out keeping the distance between two probes 2mm. The output

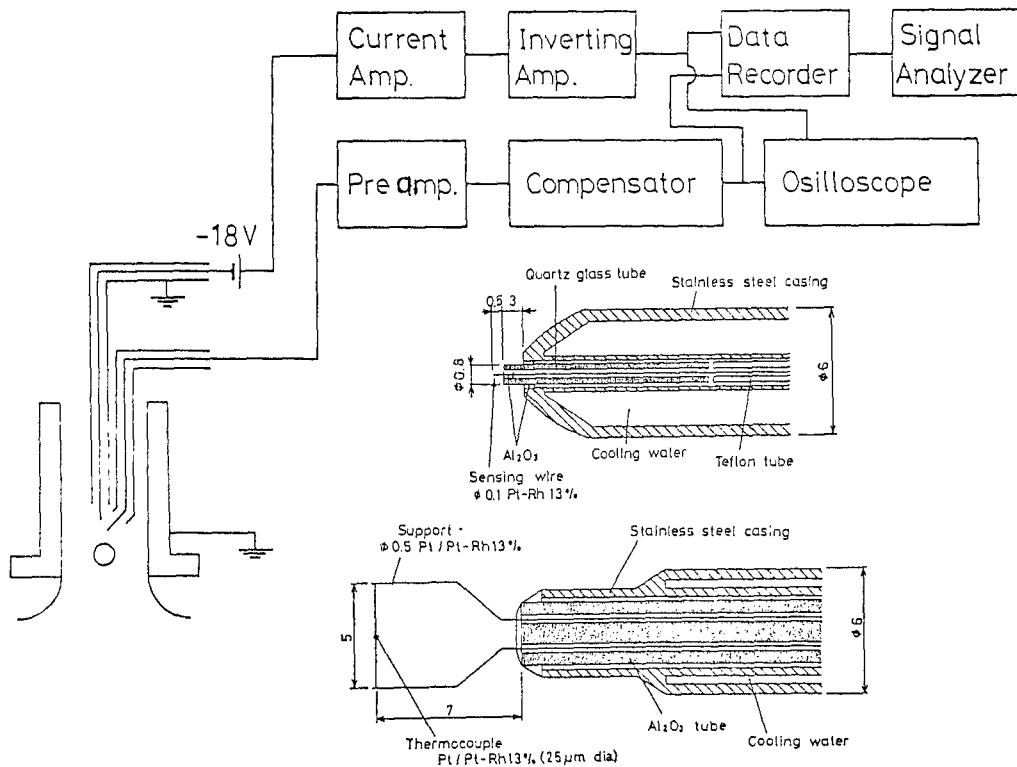


Fig. 2 Measuring system and probes

signals were recorded by a data recorder and a signal analyzer was used for statistical treatments of them.

Flow conditions of the studied flames are tabulated in Table 1, which shows the variations in velocity, approach turbulence intensity, and equivalence ratio reference to the flame No. 1.

### 3. Results and Discussion

#### 3.1. Flow Visualization

Since the local turbulence intensity in flames is not measured in the present experiment, only the approach turbulence intensities without cylinder and combustion are shown for the reference in Table 1, which were measured by a hot wire anemometer at the cross section of  $x=0\text{mm}$ .

Spark schlieren photographs of flames tabulated in Table 1 are shown in Fig. 3. A recirculating flow of high temperature burnt gas is formed in the wake of the cylinder. Two dimensional vortices of coherent structure dominate the shear layer formed between the recirculating flow and the unburnt mixture separated from the cylinder. The coherent structure appears both sides of  $x$ -axis symmetrically, and mixing and combustion proceed by the motion of engulfment of vortices. Sizes of vortices increase with distance first, and the growth of vortices and the engulfment become insignificant downstream. As the coherent structure breaks down, propagating flames in three dimensional random turbulence come out. In upstream region several coherent vortices form a group and behave an irregular periodic motion as is seen in Fig. 3

(a), which is also thought to be an effective factor of blowout judging from the records of high speed schlieren movies, though it is suggested that the motion of coherent vortices play an essential role in the process of blowout<sup>(8)</sup>.

From the observations mentioned above, flames are divided into two categories; one is a flame with coherent structure which appears in the shear layer around the recirculation zone, the other is a propagating flame in random turbulence of downstream region.

The spread of flame decreases and coherent

structure breaks down slightly earlier as flow velocity increases, but other tendencies described above do not change. The coherent structure breaks down quite earlier, when approach turbulent intensity increases, and the spread of flame increases in the downstream. The effect of coherent structure remains considerably in the downstream region when the equivalence ratio approaches the lean blowout limit, because combustion reaction in downstream becomes weak.

Table 1 Flow conditions of flames

No.		1	2	3	4
$U$	m/s	5	11	5	5
$\phi$		0.8	0.8	0.8	0.65
Turbulence grid		Type I	Type I	Type II	Type I
$u'/U$	%	1.01	0.82	1.24	1.01
$Re$ No.		$6.4 \times 10^3$	$1.4 \times 10^4$	$6.4 \times 10^3$	$6.4 \times 10^3$

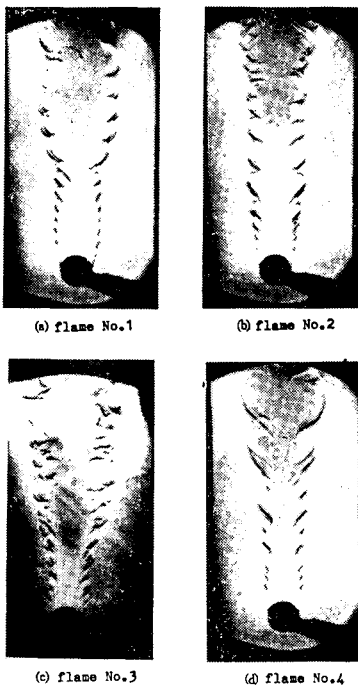


Fig. 3 Schlieren photographs of flames

### 3.2. Temperature and Ion Concentration

In order to investigate the structure of two types of flames classified in the previous section, measurements of fluctuating temperature and ion concentration have been made. From the measurements using  $Na^+$  flame reaction technique, the length of the recirculation zone was found to be approximately 50mm for any flames in Table 1. Therefore, two reference cross sections with and without recirculation zone are selected for the comparison; one is  $x=40$ mm and the other is  $x=100$ mm, respectively.

Figure 4 shows time-averaged temperature profiles and RMS values in the two cross sections. As for the flame No. 1, the time-averaged temperature profile shows a saddle shape in  $x=100$ mm owing to the heat loss from the burnt gas around the symmetry axis in the up stream. On the other hand, it reaches its maximum at

the symmetry axis in  $x=40\text{mm}$ . However, its maximum level is slightly lower than that in  $x=100\text{mm}$ , which is ascribed to the imperfect combustion in the recirculation zone depending on the state of turbulence there. The profiles of RMS values have a peak in both cross sections around the center of the time mean reaction region, where the time-averaged temperature gradient reaches its maximum.

For the flame No. 2, the same trends are observed, though the width of mixing layer and the spread of flame are decreased. The temperature difference around the  $x$ -axis in the two cross section diminishes for the flame No. 3. This is achieved by the reactedness of the recirculation zone because the increase in approaches turbulent intensity accelerates the coherent structure to break down earlier and changes the

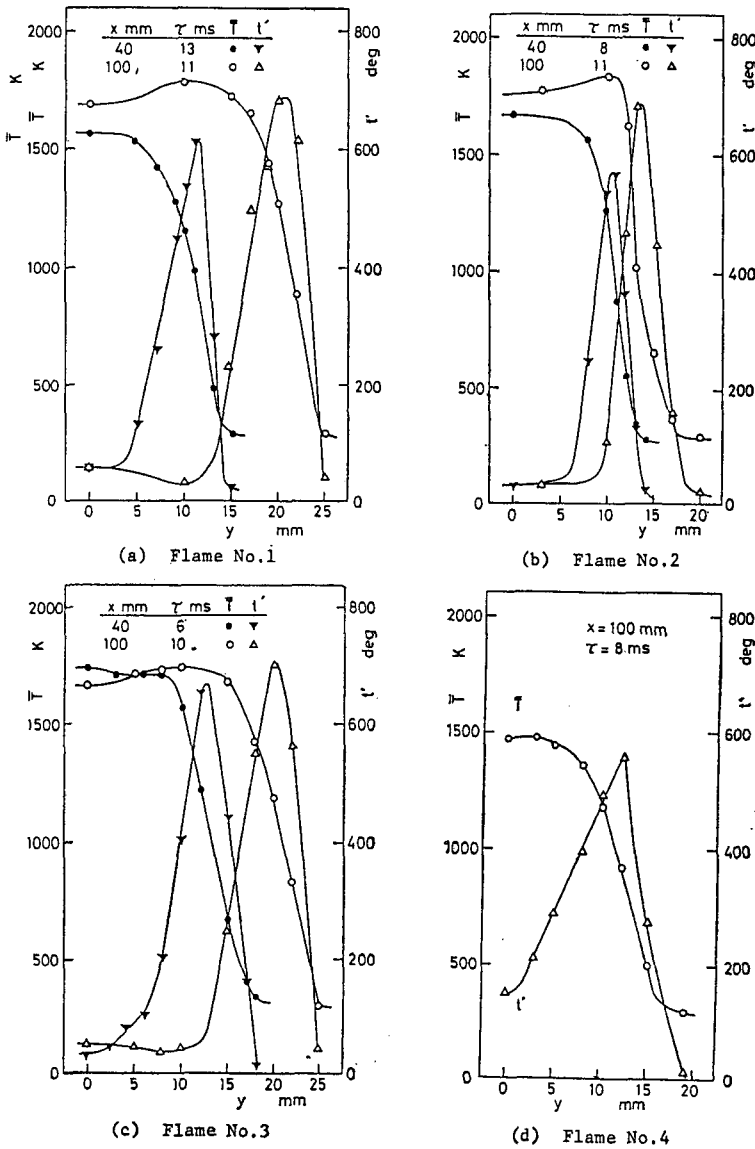


Fig. 4 Time-averaged temperatures and RMS values of fluctuations

state of mixing in the recirculation zone. Since the flame No. 4 becomes unstable and often blows out when measuring probes are inserted into the recirculation zone, measurements were made only in the cross section of  $x=100\text{mm}$ . In this case, considerable temperature fluctuations exist even around the symmetry axis, which suggests that unburnt mixture is often drawn deep into the recirculation zone and unmixedness remains around the axis.

Probability density functions (PDF) of tem-

perature fluctuations for the reference flame No. 1 are shown in Fig. 5. PDF exhibits a bimodal profile having its peaks corresponding the room temperature and burnt gases in the reaction region, though a single peaked PDF appears in both fully burnt and unburnt side. A careful comparison between the two cross sections reveals that the probabilities of intermediate temperature are quite low in  $x=100\text{mm}$ , and that the moderate probability of intermediate temperature, however, appears in  $x=40\text{mm}$ , although

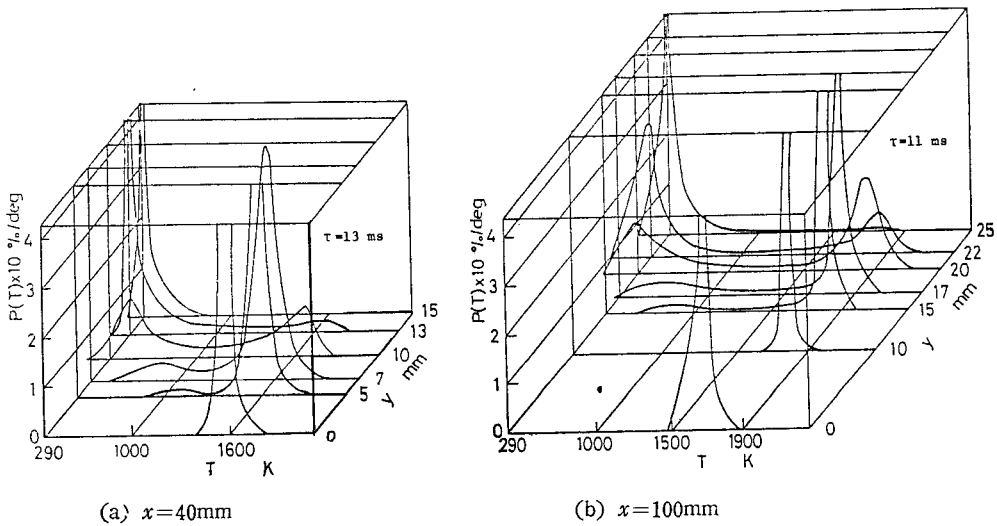


Fig. 5 PDF of temperature fluctuations for flame No. 1

the underlying profiles of PDFs are bimodal. Accordingly, the flame structure of propagating flame in random turbulence of downstream region is that gaseous parcels of unburnt mixture and burnt mixture and burnt gas get in touch with each other having a thin reacting layer between them, that is, a wrinkled laminar flame or laminar flamelets. On the other hand, another structure in which fine eddies of various reactedness as well as burnt and unburnt gases are included appears in the flames with coherent structure in the upstream shear layer. Since high speed schlieren movies show that there is the part subjected a strong stretch around the

trailing edge of the engulfment of coherent vortex, as shown in Fig. 6 schematically, the structure is supposed to be a "distributed reaction

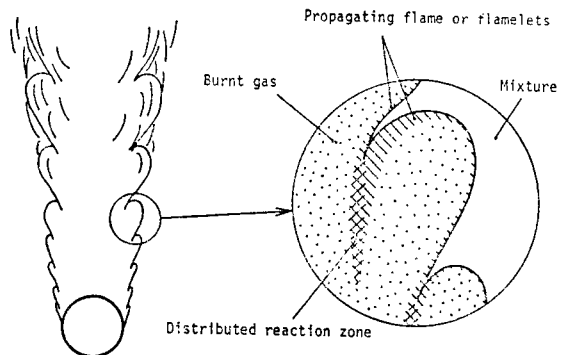


Fig. 6 Schematic image of a flame with coherent vortex

zone<sup>”(16)</sup> where fine scale eddies of various reactedness prevail. Therefore, the flame with coherent structure in the shear layer has the structure consisting of a wrinkled laminar flame and partly a distributed reaction zone.

Figure 7 shows PDFs of ion current fluctuations. In the cross section of  $x=100\text{mm}$ , profiles of  $y=17\sim 22\text{mm}$  have three peaks corresponding the unburnt gas (null), burnt gas(low) and reacting zone(high), which are typical for a wrinkled laminar flame. On the other hand, such a profile with significant three peaks is not seen in  $x=40\text{mm}$ . This is supposed to be one of the proofs insisting that eddies of various reactedness exist in this region. These facts are consistent with those suggested by the PDFs of fluctuations of temperature and ion current, combustion reaction almost completes around the symmetry axis in the downstream region. In  $x=40\text{mm}$ , however, fairly high ion current which means the existence of combustion reaction is observed at  $y=5\text{mm}$  in the recirculation zone, and some unburnt mixture of low temperature are detected at the same location. Accordingly,

the recirculation zone is not always filled with fully burnt gases, but combustion reaction takes place intermittently in accordance with the engulfment of unburnt mixture into the recirculation zone.

Power spectra of fluctuations of temperature and ion current are shown in Fig. 8 and 9. In  $x=40\text{mm}$ , a broad peak at a frequency of 350 Hz is observed at  $y=13\text{mm}$  in the shear layer. The frequency reveals a periodic motion in large scale, that is the coherent structure in the shear layer. However, the broadness suggests the randomness of appearance frequency of coherent vortices. Any pronounced peak does not appear except in the shear layer and the dissipation in high frequency region is almost uniform. It is also supposed by the above considerations that the mixing and combustion in the shear layer formed around the recirculation zone are dominated by the motion of coherent vortices and the propagating flame in downstream region is affected by the random turbulence.

Figure 10 shows cross correlation coefficients  $R_{TI}(0, 0)$  between fluctuations of temperature

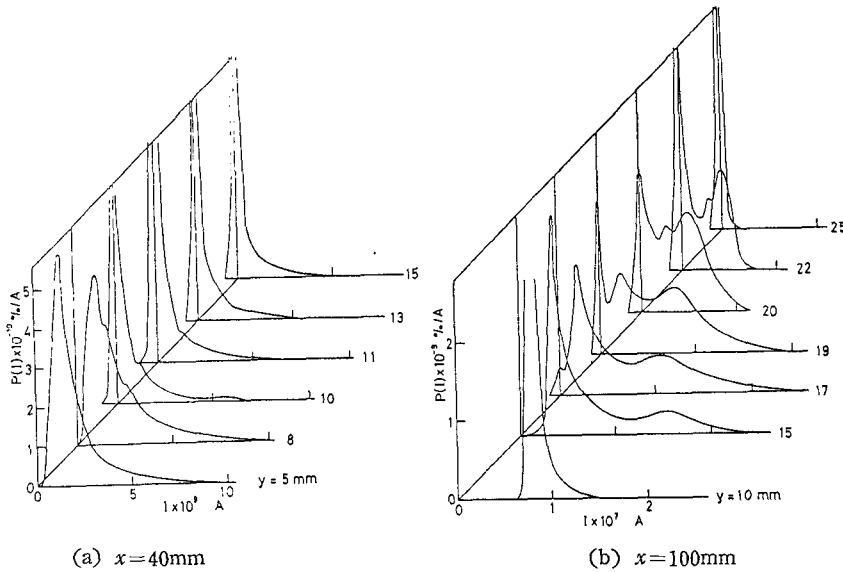


Fig. 7 PDF of ion current fluctuations for flame No. 1

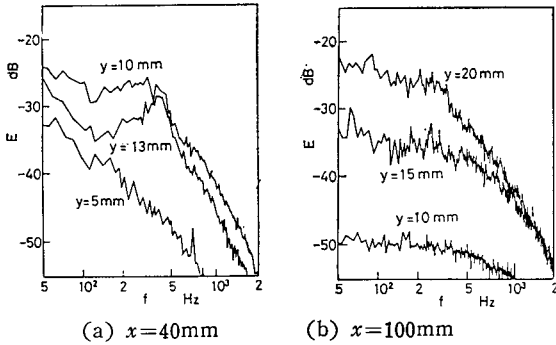


Fig. 8 Power spectra of temperature fluctuations for flame No. 1

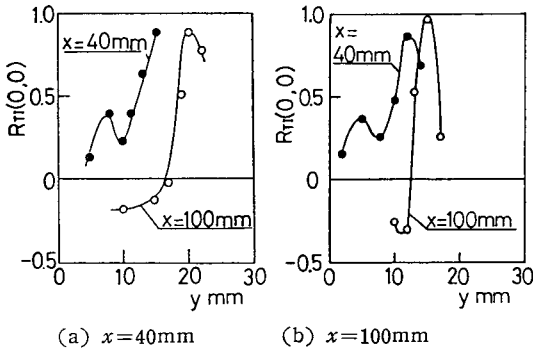


Fig. 9 Power spectra of ion current fluctuations for flame No. 1

and ion current at the same point and the same time. The measurements were carried out inserting two probes into a flame simultaneously. The cross correlation  $R_{Ti}(\Delta x, \Delta t)$  is defined by the relation

$$R_{Ti}(\Delta x, \Delta t) = \{T(x, t) \cdot I(x + \Delta x, t + \Delta t)\} / [\{\overline{T^2(x, t)} \cdot \overline{I^2(x + \Delta x, t)}\}^{1/2}]$$

where  $\Delta x$  is the distance between two probes and  $\Delta t$  is the time lag. In the present study, the cross correlation coefficients at the same point and the same time were obtained by compensating the small time lag caused from the fact that  $\Delta x$  equals 2mm. In the cross section of  $x=100\text{mm}$ , the values of  $R_{Ti}(0, 0)$  are negative in the burnt gas side of the time mean reaction region ( $y=10\sim 15\text{mm}$ ) and become positive in the unburnt side of it. This fact means

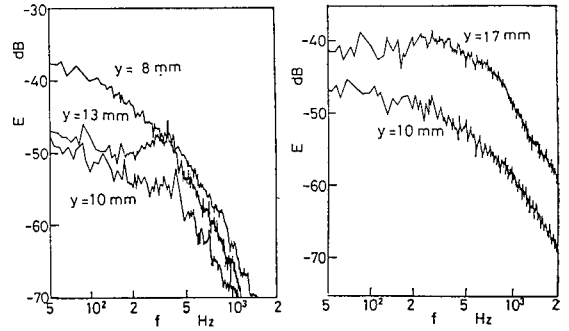


Fig. 10 Variation of cross correlation coefficient

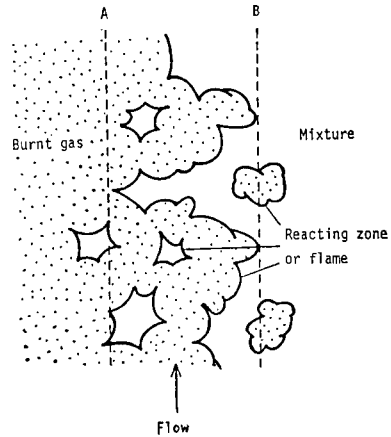


Fig. 11 Schematic image of a propagating flame

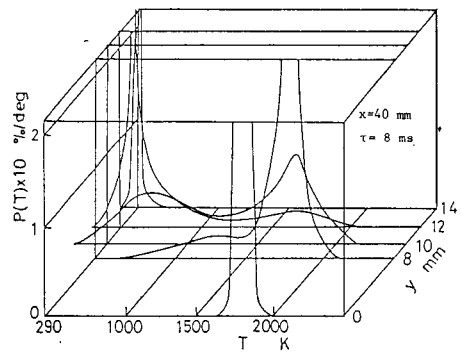


Fig. 12 PDF of temperature fluctuations for flame No. 2

that the increment of ion current, that is combustion reaction, is accompanied with plunging cold gas parcels in the burnt side. If the flame



structure is a wrinkled laminar flame or laminar flamelets in which combustion reaction takes place at the thin interfaces of parcels of burnt and unburnt gases, as shown in Fig. 11 schematically, it is quite comprehensible that the measurements at two locations *A* and *B* exhibit the trend in correlation described above. In  $x=40\text{mm}$ , the values of  $R_{TI}(0,0)$  always positive and show a somewhat different trend in the burnt side(the recirculation zone side). It is supposed that unburnt mixture does not exist as parcels there and the imperfect mixing zone of fine scale is formed. This is supported by the local existence of distributed reaction zone in Fig. 6. In order to confirm the above concept, the same measurements were carried out for the flame No. 2. The apparent tendencies of the cross correlation coefficients are quite the same, though the higher velocity has changed the position and width of time mean reaction zone.

### 3.3. Effects of Velocity

PDFs of temperature fluctuations for the flame No. 2 are shown in Fig. 12. The same features

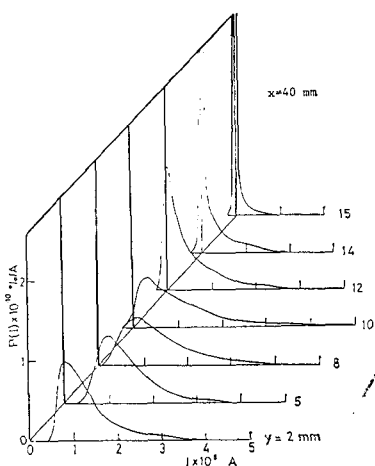


Fig. 13 PDF of ion current fluctuations for flame No. 2

as the flame No. 1 are prominent in this case of higher flow velocity. PDFs exhibit typical bimodal profiles in downstream and considerable provability of intermediate temperature is observed in upstream. Corresponding PDFs of ion current fluctuations in Fig. 13 show single peaked profiles in the shear layer and the recirculation zone, although they have three peaks in downstream reaction zone. The significant eddies of intermediate reactedness in the recirculation zone are detected when the flow velocity increases. This is because the increase shear force in the shear layer creates more distributed reaction zone and enhances the unmixedness in the recirculation zone.

### 3.4. Effect of Approach Turbulence Intensity

PDFs of temperature and ion current fluctuations in the cross section of  $x=40\text{mm}$  for the flame No. 3 are shown in Figs. 14 and 15. As mentioned in the section of flow visualization, the coherent structure breaks down rapidly and loses its two dimensionality already in  $x=40\text{mm}$  as the approach turbulence intensity is increased. The features of PDFs in the outer part of the shear layer ( $y=8\sim 15\text{mm}$ ) reveals that the flame structure is a like the one in propagating flames

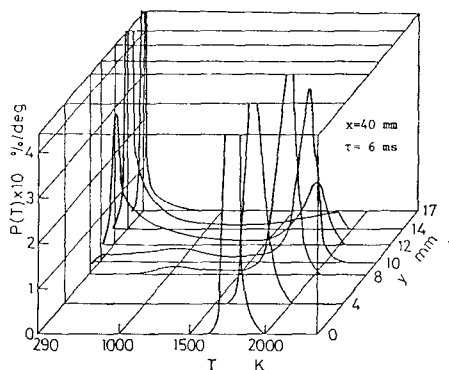


Fig. 14 PDF of temperature fluctuations for flame No. 3

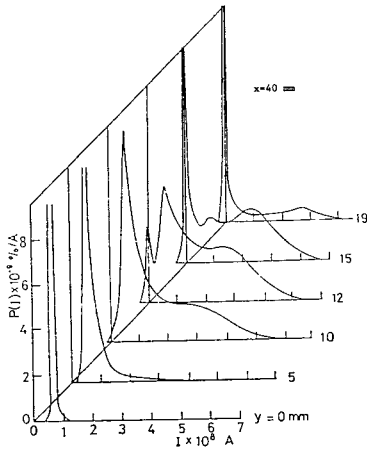


Fig. 15 PDF of ion current fluctuations for flame No. 3

in downstream. However, PDFs of temperature and ion current at  $y=10\text{mm}$  indicate the existence with various reactedness. Profiles of PDFs which indicate the existence of combustion reaction or unburnt mixture are not observed inside the recirculation zone and the reactedness of the recirculation zone become higher comparing with the flame No. 1. Accordingly, time-averaged temperature inside the recirculation zone increases, which is expected to improve the stability of flames.

3.5. Effects of Equivalence Ratio

The spread of propagating flames in downstream is obstructed by the deterioration in burning velocity when the equivalence ratio of mixture approaches the lean blowout limit. Although large scale vortex motions originated in coherent structure are prominent even in the downstream cross section of  $x=100\text{mm}$  from the records of optical observations characteristics suggested by the PDFs in Figs. 16 and 17 indicate the same structure as those of other flames in downstream. Therefore, the inner structure

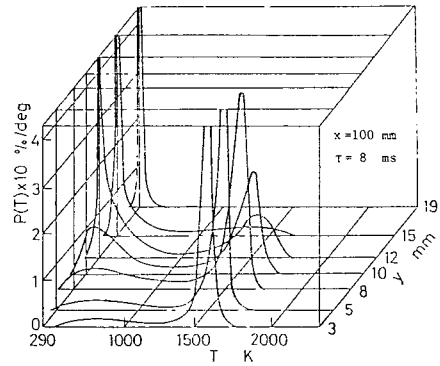


Fig. 16 PDF of temperature fluctuations for flame No. 4

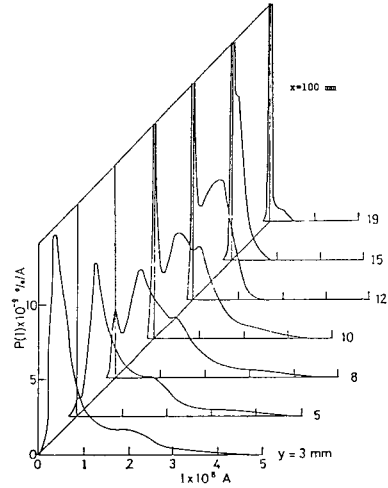


Fig. 17 PDF of ion current fluctuations for flame No. 4

of large vortices is considered to be a wrinkled laminar flame or laminar flamel. Some unburnt mixture or unmixedness remains around the symmetry axis because of the weakness of combustion reaction.

4. Conclusions

(1) A flame with coherent structure appears in the shear layer formed around the recirculation zone behind the cylinder, and a propagating flame in random turbulence spreads in downstream.

(2) A bimodal PDF of temperature fluctuations and a three peaked PDF of ion current fluctuations are typical for a propagating flame in downstream. The features correspond to the flame structure of a wrinkled laminar flame or laminar flamelets in which gaseous parcels of unburnt mixture and burnt gas get in touch with each other having a thin reacting layer between them.

(3) Macroscopic mixing of the flame with coherent structure is dominated by the behavior of coherent vortices, and the flame has the structure consisting of a wrinkled laminar flame and partly a distributed reaction zone which appears at the part subjected a strong stretch. An imperfect mixing of fine scale eddies of various reactedness prevails the distributed reaction zone.

(4) Higher flow velocity creates more distributed reaction zone by a stretch of strong shear force. Higher approach turbulence intensity accelerates the coherent structure to break down earlier. Low equivalence ratio obstructs the spread of propagating flames.

### References

- (1) Williams, G.G., Hottel, H.C., and Scurlock, A.C., and Scurlock, A.C., "Flame Stabilization and Propagation in High Velocity Gas Streams," Proceedings of the Third Symposium on Combustion, Williams and Wilkins, pp.21~40, 1949
- (2) Zukoski, E.E., and Marble, F.E., "Experiments Concerning the Mechanism of Flame Blowoff from Bluff Eddies," Proceedings of the Gas Dynamics Symposium on Aerothermochemistry, Northwestern University, pp.205~210, 1956
- (3) Cheng, S.I., and Kovitz, A.A., "Theory of Flame Stabilization by a Bluff Body", Proceedings of the Seventh Symposium (International) on Combustion, Butterworths, pp.681~691, 1959
- (4) Wright, F.H., and Zukoski, E.E., "Flame Spreading from Bluff-Body Flameholder," Proceedings of the Eighth Symposium (International) on Combustion, Williams and Wilkins, pp.933~943, 1962
- (5) Winterfeld, G., "On Processes of Turbulent Exchange Behind Flame Holders," Proceedings of the Tenth Symposium (International) on Combustion, The Combustion Institute, pp.1265~1275, 1965
- (6) Davies, T.W., and Berr, J.M., "Flow in the Wake of Bluff-Body Flame Stabilizers," Proceedings of the Thirteenth Symposium (International) on Combustion, The Combustion Institute, pp.631~638, 1971
- (7) Katsuki, M., and Mizutani, Y., "Flame Stabilization Behind a Bluff-Body Flame Holder," Technology Reports of the Osaka University, Vol. 27, No. 1385, pp.495~505, 1977
- (8) Tsuji, H., "Combustion Phenomena," Science of Machine, Vol. 29, No. 9, pp.1123~1128, (In Japanese) 1977
- (9) Keller, J.O., Vaneveld, L., Korschelt, D., Hibbard, G.L., Goniem, A.F., Daily, J.W., and Oppenheim, A.M., "Mechanism of Instabilities in Turbulent Combustion Leading to Flashback," AIAA Journal, Vol. 20, No. 2, pp.00~00, 1982
- (10) Yamaguchi, S. Ohiwa, N., and Hiramatsu, K., "Study on Premixed Flames Stabilized by Multi-Rod Bluff-Bodies," Preprints of the 18th Combustion Symposium of Japan, The Combustion Institute of Japan, pp.4~6, (in Japanese) 1980
- (11) Lewis, K.J., and Moss, J.B., "Time-Resolved Scalar Measurements in a Confined Turbulent Premixed Flame." Proceedings of the Seventeenth Symposium (International) on Combustion, The Combustion Institute, pp.267~277, 1979
- (12) Pitz, R.W., and Daily, J.W., "Experimental Study of Combustion in a Turbulent Free Shear Layer Formed at a Rearward Facing Step," AIAA Paper, No. 81-0106, 1981
- (13) Kunugi, M. and Jinno, H., "Measurement of Fluctuating Temperature," Proceedings of the Seventh Symposium (International) on Combustion

- stion, The Combustion Institute, pp.942~948, 1959
- (14) Shepard, C.E., and Warshawsky, I., "Electrical Techniques for Compensation of Thermal Time Lag of Thermocouples and Resistance," NACA-TN-2703, 1952
- (15) Yoshida, A., and Gunther, R., "Experimental Investigation of Thermal Structure of Turbulent Premixed Flames," Combustion and Flame, Vol 38, pp.249~258, 1980
- (16) Summerfield, M., Reiter, S.H., Kebely, V., and Mascolo, R.W., "The Structure and Propagation Mechanism of Turbulent Flames in Flames in High Speed Flow," Jet Propulsion, Vol. 25, No. 8, pp.377~384, 1955